Hydrol. Earth Syst. Sci. Discuss., 12, 569–608, 2015
www.hydrol-earth-syst-sci-discuss.net/12/569/2015/
doi:10.5194/hessd-12-569-2015

Hydrology and Earth System Sciences
Open Access
Discussions

High-resolution estimation of the water balance components from high-precision lysimeters

M. Hannes[1,3], U. Wollschläger[2,3], F. Schrader[4,5], W. Durner[4], S. Gebler[6], T. Pütz[6], J. Fank[7], G. von Unold[8], and H.-J. Vogel[1,3]

[1]Helmholtz Centre for Environmental Research GmbH – UFZ, Theodor-Lieser-Straße 4, 06120 Halle, Germany
[2]Helmholtz Centre for Environmental Research GmbH – UFZ, Permoserstr. 15, 04318 Leipzig, Germany
[3]WESS – Water and Earth System Science Competence Cluster, Keplerstraße 17, 72074 Tübingen, Germany
[4]Institute of Geoecology, Soil Science and Soil Physics, Technische Universität Braunschweig, Langer Kamp 19c, 38106 Braunschweig, Germany
[5]Thünen Institute of Climate-Smart Agriculture (TI-AK), Bundesallee 50, 38116 Braunschweig, Germany
[6]Agrosphere (IBG-3), Institute of Bio- and Geosciences, Forschungszentrum Jülich GmbH, 52425 Jülich, Germany
[7]Joanneum Research – Resources, Elisabethstraße 18/2, 8010 Graz, Austria

[8]UMS GmbH, Gmunder Str. 37, 81379 München, Germany

Received: 21 October 2014 – Accepted: 14 December 2014 – Published: 14 January 2015

Correspondence to: M. Hannes (matthias.hannes@ufz.de)

Published by Copernicus Publications on behalf of the European Geosciences Union.

Abstract

Lysimeters offer the opportunity to determine precipitation, evapotranspiration and groundwater-recharge with high accuracy. In contrast to other techniques, like Eddy-flux systems or evaporation pans, lysimeters provide a direct measurement of evapotranspiration from a clearly defined surface area at the scale of a soil profile via the built-in weighing system. In particular the estimation of precipitation can benefit from the much higher surface area compared to typical raingauge systems. Nevertheless, lysimeters are exposed to several external influences that could falsify the calculated fluxes. Therefore, the estimation of the relevant fluxes requires an appropriate data processing with respect to various error sources. Most lysimeter studies account for noise in the data by averaging. However, the effects of smoothing by averaging on the accuracy of the estimated water balance is rarely investigated. In this study, we present a filtering scheme, which is designed to deal with the various kinds of possible errors. We analyze the influence of averaging times and thresholds on the calculated water balance. We further investigate the ability of two adaptive filtering methods (the Adaptive Window and Adaptive Threshold filter (AWAT-filter) (Peters et al., 2014) and the consecutively described synchro-filter) in further reducing the filtering error. On the basis of the data sets of 18 simultanously running lysimeters of the TERENO SoilCan research site in Bad Lauchstädt, we show that the estimation of the water balance with high temporal resolution and good accuracy is possible.

1 Introduction

The determination of water fluxes across the boundary layer between soils, plants and atmosphere and their temporal dynamics is of fundamental importance for the understanding of the water and energy balance. While it is challenging to obtain direct measurements of these fluxes in the field, lab measurements are restricted to small systems and artificial boundary conditions. Modern lysimeters offer the possibility of measuring the relevant fluxes of natural soils under atmospheric boundary conditions and are therefore often seen as tools for bridging the gap between lab and field measurements. Lysimeters have a long tradition of measuring groundwater recharge (Robison et al., 2004). Their ability of measuring also water fluxes at the soil-atmosphere interface was soon recognized (Young et al., 1996). Today, high-precision weighing systems make modern lysimeters an ideal measurement tool for both demands (Fank and von Unold, 2007). The high temporal resolution of modern lysimeter measurements allows investigations of detailed processes at the soil-plant-atmosphere interface.

However, the derivation of accurate fluxes with high precision from lysimeter-measurements requires an adequate data processing due to multiple sources of errors affecting the measurement systems. Besides weighing system errors, measurements of field lysimeters are exposed to several external influences. External errors are, for example, vibrations induced by wind or field work, mass changes due to animals like mice or birds, influences due to sampling from the seepage water reservoir. Therefore, a preceding filtering procedure for the measured data is mandatory to evaluate the fluxes with high accuracy.

Although the determination of fluxes from the weighing data is straightforward, precipitation (P) and evapotranspiration (ET) have to be separated in an indirect way. Positive fluxes at the soil-atmosphere-interface are interpreted as P and a negative fluxes as ET, assuming that these processes do not ocuur simultanously. This algorithmic separation can lead to large errors in the calculated individual fluxes, if noise-induced oscillations are not filtered from the data and therefore are interpreted as P or ET fluxes. Even though, for some applications (e.g. for modeling bare soils) it may be sufficient to know only the net flux at the soil-atmosphere interface. The differentiation between P and ET is essential, when transpiration processes come into play. This is due to the fact, that for soils covered by vegetation, the major part of ET is lost by transpiration, and this water is removed via root water uptake from deeper regions of the soil. A mixing of surface and subsurface fluxes would lead to errors when modelling these processes.

A common method to remove the noise is a smoothing of the data with a static or a moving mean. Although widely applied in literature, the effects of smoothing and averaging on the accuracy of the estimated fluxes are rarely discussed. For example, Meissner et al. (2007) investigated the ability of lysimeters measuring small changes in water storage considered as dew and rime with a temporal resolution of one hour. In contrast, Nolz et al. (2013a) report wind influences on the weighing signal and suggest an averaging time of 30 min. In their recent studies (Nolz et al., 2013b, 2014), smoothing is done with a natural cubic spline and manually adjusted smoothing factors. While an enlargement of the smoothing time window leads to a reduction of noise effects (noise error), the temporal resolution is reduced and an increasing part of the precipitation is lost due to a mixing with evapotranspiration (mixing error). Considering this issue, Vaughan et al. (2007) present a filtering method that is based on the fitting of the mass curve. However, their investigation is based on a data set with a time resolution of 1 h and the process details are further reduced by the fitting algorithm. In their study from 2009 (Vaughan and Ayars, 2009) data smoothing is done with a Savitzky–Golay-filter operating over a time period of a minimum of one hour. First steps in investigating filtering schemes for evaluating highly resolved components of the water balance on the basis of synthetic data were presented by Schrader et al. (2013) discussing the issue of falsifying fluxes by large averaging times. Recently, Peters et al. (2014) proposed a filtering algorithm for lysimeter weighing data to obtain temporally higher resolved data by adapting the used filtering parameters according to the signal strength. Despite these efforts of developing adequate strategies for retrieving the water balance with high accuracy and high temporal resolution, the influence of these filtering approaches on the accuracy and resolution on a basis of real data sets is still hardly investigated. However, for integrating evapotranspiration data from lysimeters into larger-scale hydrologic or climate models, adequate filtering algorithms are essential to provide the required data accuracy. Furthermore, the relevance of short-term rain events with a duration below one hour but high precipitation rates is well known. This

HESSD
12, 569–608, 2015

is relevant not only for floodforcasting but also for the wetting behaviour of the soil (e.g. Grunow, 1960; Forster and Baumgartner, 1999).

This study is motivated by the following two questions: (i) what accuracy of the water balance can be achieved at a temporal resolution in the subhour regime (15 min), and (ii) to what extend do the choice of the filtering parameters or the use of more elaborate adaptive methods influence this accuracy? We first present a comprehensive processing scheme, which accounts for the different error types on the lysimeter weighing data. We then analyze the effects of the filtering parameters for noise reduction on the calculated fluxes. We further investigate the ability of two adaptive methods (the Adaptive Window and Adaptive Threshold (AWAT) filter (Peters et al., 2014) and the consecutively described synchro-filter) in further reducing the filtering error. To differentiate between the effects of the noise error and the mixing error, we split our data into subsets, where only one of both effects is relevant. For our investigations, we use data sets from 18 high-precision lysimeters covering a period of two months. All lysimeters are located at the experimental station Bad Lauchstädt, which is part of the TERENO SoilCan network in Germany (Pütz et al., 2011; Zacharias et al., 2011). This set of parallel lysimeters can be considered as real replicates, as they are exposed to the same atmospheric boundary condition. Thus, they provide information on the robustness of the filtering approach and, moreover, errors that are difficult to distinguish from real events can be identified.

2 Material and methods

2.1 Data aquistion

The lysimeters used for this study are part of the TERENO SoilCan project. In the framework of the TERestrial ENvironmental Obervatories (TERENO), a network of observatories has been set up to explore long-term impacts of climate and land use change on a regional level (Bogena et al., 2006; Zacharias et al., 2011). Following this idea, the TERENO SoilCan project comprises a total of 126 lysimeters that are distributed over 13 sites throughout Germany (Pütz et al., 2011).

The lysimeters of the SoilCan network are arranged in hexagons of six lysimeters (consecutively indicated by L1, L2, ...) at one plot. Figure 1 shows a schematic drawing of the lysimeter configuration. Each of the lysimeters has a circular surface of 1 m^2 area and a depth of 1.5 m. The lysimeters are equipped with different sensors for measuring matric potential at 10, 30, 50 and 140 cm below the ground surface. The volumetric soil water content is measured with TDR sensors at three different depths (10, 30, 50 cm). Further measurements of CO_2 concentration, soil heat flux and net radiation are conducted continuously. The matric potential at the lower boundary is controlled by a set of suction cups, such that water can be pumped into and out of the lysimeter. An automatic pumping system is used to adjust the pressure head at the lower boundary to the value of three reference tensiometers installed in the field. The lysimeters are equipped with a weighing system that allows a resolution of 10 g (respectively 0.01 mm) for measuring the mass of the lysimeter, and 1 g for recording the mass of the seepage water reservoir. The mass data we refer to as raw data or signal was internally aquired at a frequency of 0.2 Hz (5 s), averaged with a moving mean over 6 of these 5 s values and logged with a frequency of 1 min^{-1}.

At the research site in Bad Lauchstädt, three hexagons (here indicated by BL1, BL2, BL3) with a total of 18 lysimeters were set up. Two hexagons (12 lysimeters) are cultivated with crops (BL1 and BL2). In the period of the presented data set, the grown crop was winter rape. The other 6 lysimeters are covered with grass. For each hexagon, the soils originate from two different locations in Germany. Therefore, in Bad Lauchstädt, we can investigate six different soil textures from six different locations, each location represented with a total of three lysimeters. For the evaluation of the filtering algorithms, we used the data sets of all the 18 lysimeters for a period of two month in spring 2013.

2.2 Basic processing scheme

Lysimeters are always directly exposed to environmental conditions and therefore prone to multiple error sources. The determination of an accurate time-resolved water balance requires an adequate data processing to eliminate these influences. From our experience, a proper processing scheme should include five major steps, which are listed in Fig. 2.

The threshold filter and the smoothing filter are described in detail by Schrader et al. (2013) and will therefore only be shortly addressed. To this basic scheme we added a manual filter, a median filter and an oscillation threshold filter as further components, which we consider as essential for the determination of temporally highly resolved fluxes using lysimeter data. It is important to conduct the filtering in the suggested sequence. In particular the filtering of discrete events (filter steps 1–3) has to be done prior to the filtering of noise (4–5). Otherwise, distinct events will be blurred by smoothing and cannot be filtered effectively afterwards.

Apart from the first filter step (manual filter) all the filter steps are applied to the mass of the seepage water tank, corresponding to the seepage water flux, as well as to the summarized mass of lysimeter and seepage, corresponding to the flux at the soil-atmosphere interface (P and ET). Only the manual filter is applied to the mass data sets of the seepage water tank and the lysimeter (before summarizing it). The threshold filter is first applied to the seepage mass data, to eliminate possible spikes in the data (especially due to automatic emptying) before calculating the sum of lysimeter and seepage mass.

2.2.1 Manual filter

After a step of pre-processing, which may include interpolation or filling of missing data points if necessary, a manual filter should be the first step in data processing. It is used to remove defective data periods. The most common error sources in this respect are heavy external influences affecting the weighing data, which are e.g. caused by har-

HESSD
12, 569–608, 2015

vesting, maintenance or measurements on the lysimeters. The influence of such forces on the weighing data can be very strong (or hard to recognize in other manners), so that the subsequent filtering algorithm will not succeed in removing these errors. It may also be feasible, to determine heavily affected time periods by checking the automatically processed results. In the presented data set, we exposed a manual filtering for some hours at three different days with known maintenance and at two further periods, where one single lysimeter showed distinct outliers in the data. During these periods, there was no precipitation and the weighing data was interpolated to fill the measurement gaps. The effect of the manual filter is illustrated in Fig. 3b compared to raw data (Fig. 3a).

2.2.2 Threshold filter

The threshold filter has the capability of removing strong and short external influences from the data set. Typical error sources are mass changes during automatic emptying of the seepage water storage tanks, humans or (heavy) animals stepping on the lysimeter or malfunctions in data transfer. By defining thresholds for the maximum possible precipitation, evapotranspiration and the maximum mass change in the seepage water reservoir, the filter can detect physical unrealistic fluxes. These data points are removed and substituted by linear interpolations. Small errors, caused by wind effects or, for instance, by small animals, cannot properly be removed from the data at this stage because the filter threshold should not undershoot high, but still reasonable water fluxes. The description of the parameter selection is given in Sect. 2.3.1. An example for the benefit of the threshold filter is illustrated in Fig. 3c.

2.2.3 Median filter

While the threshold filter is a suitable tool to eliminate large errors, influences, that lead to only small mass changes (like small animals, wind, temperature-effects, signal noise . . .) are not removed. The first step for a reduction of these errors is the applica-

HESSD
12, 569–608, 2015

tion of a median filter that eliminates short-term spikes from the data set that are below the limits of the threshold filter. The effect of the median filter is illustrated in Fig. 3d. This filter is a very effective amendment to the threshold filter for eliminating discrete errors. As described in Sect. 2.3.1 we use a time window of 15 min for the calculation of the median.

2.2.4 Smoothing filter

While the previous filter steps are designed to eliminate discrete errors, the last two filter steps are designed to deal with remaining diffuse noise. The primary step in removing noise is a smoothing filter, where different smoothing algorithms can be used. Schrader et al. (2013) discussed the application of a second degree Savitzky–Golay filter (which is based on a polynomial approximation) as well as the simple moving average which both show different advantages and disadvantages for the application of lysimeter data. The overall issue of such smoothing filters is the blurring of short-time effects and the mixing of ET and P. To avoid temporal distortion or even elimination of short-term events, it is advisable to restrict smoothing to a short time period. In our calculations, we used the simple moving average with a time window of $n = 15$ min, to restore a high temporal resolution and to avoid distinct blurring effects (see Sect. 2.3.1). The moving average calculates the arithmetic mean of the data points in the time window $t_{i-(n-1)/2}$ to $t_{i+(n-1)/2}$ for each data point at time t_i. Figure 3e gives an illustration of the effect of the smoothing filter.

2.2.5 Oscillation threshold filter

Smoothing filters are not able to eliminate all fluctations, especially when they are limited to short time windows to retain a high temporal resolution and to preserve short term effects. In situations where the external forcing (precipitation or evapotranspiration) is low or vanishing, remaining noise will falsify the calculated fluxes. Figure 3f illustrates the issue of remaining noise components in the calculated fluxes before and

HESSD
12, 569–608, 2015

after the use of the oscillation threshold filter. Although the oscillatory fluxes are small, they may lead to noticeable deviations in the cumulative values of precipitation and evapotranspiration.

One way of filtering these oscillations would be a simple threshold algorithm, where only fluxes, that exceed a certain threshold are considered as real fluxes. This technique has the disadvantage, that slow changes (during evapotranspiration, light rain, dew or snowfall) will not be registered. To avoid this problem, our algorithm ensures that also slow processes will be recognized as long as their contribution in a sum exceeds the defined threshold. Starting from an initial data point, this algorithm determines the next point in time where the cumulative mass change exceeds a predefined threshold. When this threshold is reached, the intermediate data points are lineraly interpolated:

$$M_k = M_i + \frac{M_l - M_i}{t_l - t_i} \cdot (t_k - t_i), \text{ for } i < k < l - 1. \quad (1)$$

In this formula, M is the sum of the masses of the lysimeter and the seepage water tank at time t, k indicates the starting point, and l the first point, where the threshold has been exceeded. Small fluctuations that are not due to real fluxes are eliminated. The oscillation threshold filter enables the registration of slow processes such as light rain events, snowfall or evapotranspiration, if they are lasting long enough to exceed the threshold as a sum. The functioning of this algorithm is illustrated in Fig. 3f. Nevertheless, processes with a low flux rate and a short duration – such that the threshold is not reached – are still not registered and they fall out of the precision range defined by the oscillation threshold. Thus, the threshold value defines the limit of processes that cannot further be resolved because they cannot be distinguished from the remaining noise. The choice of the oscillation threshold value is discussed in Sect. 2.3.1.

2.2.6 Calculation of fluxes

After the execution of the presented filtering steps, the fluxes can be calculated from the processed data set. The seepage flux S is simply calculated from the increase in the mass m_S of the seepage water reservoir.

$$S(t_i) = \frac{m_S(t_{i+1}) - m_S(t_i)}{t_{i+1} - t_i} \quad (2)$$

The calculation of precipitation and evapotranspiration requires a distinction of these cases. This separation implies the assumption that no evapotranspiration is occuring during rainfall events or that evapotranspiration is at least negligible.

$$J(t_i) = \frac{M_{i+1} - M_i}{t_{i+1} - t_i} \quad (3)$$

$$P(t_i) = \begin{cases} J(t_i) & \text{, if } J(t_i) >= 0 \\ 0 & \text{, if } J(t_i) < 0 \end{cases} \quad (4)$$

$$\mathrm{ET}(t) = \begin{cases} 0 & \text{, if } J(t_i) >= 0 \\ -J(t_i) & \text{, if } J(t_i) < 0 \end{cases} \quad (5)$$

Here, J indicates the mass flux at the soil-atmosphere interface, P is precipitation and ET is evapotranspiration. Additionally to the mass changes due to these water fluxes, the biomass accumulation due to plant growth also leads to a continous mass change. Using the described separation procedure, this mass change is registered as precipitation. The mass reduction due to harvesting is counted as ET. For a correct determination of the cumulative fluxes in the water balance, these fluxes have to be corrected with regarding to this effect. We refrain from a detailed discussion of this long-term aspect and focus on the filtering of short-term fluctuations in the lysimeter data.

HESSD
12, 569–608, 2015

2.3 Parameter selection and adaptive methods

2.3.1 Parameter selection

The basic processing scheme provides all the necessary components to tackle the different error sources on the lysimeter weighing data and to obtain a time-resolved water balance. However, the operator has to define some parameters, which influence the quality of the filtering and the precision of the resulting fluxes. The choice of the threshold values in filtering step 2 (threshold filter) is rather simple and can be determined by the maximal pumping rate at the lower boundary of the lysimeter, the maximal precipitation rate and the maximal ET rate including a safety factor (see also Schrader et al., 2013). The parameters that were used as standard in our calculations are listed in Table 1.

The selection of the time window for the median and the smoothing filter (filter steps 3 and 4) is much more critical. While large time windows ensure an effective reduction of noise (noise error), such large averaging times also reduce the temporal resolution of processes and lead to a progressive mixing of P and ET (mixing error), which also is an error source in the calculation of an accurate water balance. The influence of the smoothing filter and the oscillation threshold filter on the noise error and the mixing error is displayed in Fig. 4. By using the subsequent oscillation threshold filter, it is possible to shorten time periods for averaging and to retain a higher resolution of processes. Considering the high dynamics of observed precipitation events of less than 20 min in periods of high evapotranspiration (i.e. short summer rain, see also examples in Fig. 7) we recommend a time window of 15 min at maximum, which is used in our calculations. This ensures keeping a high temporal resolution of our processed data set. This window length of 15 min is also sufficient for the purposes of the median filter, which is designed to eliminate local errors of only some data points in the data and is also used for our calculations.

Finally, the only remaining parameter to choose, is the oscillation threshold value (filter step 5), which is used to remove remaining noise components from the data, while maintaining a high temporal resolution in the calculated fluxes. Figure 4a and b illustrate that a very effective elimination of noise is possible, using the oscillation threshold filter. Figure 4c shows further, that the combination of the short time smoothing together with the oscillation threshold filter leads to a better temporal reflection of the precipitation process compared to the removal of oscillations by the use of a longer averaging time. However, it can be seen, that the oscillation threshold filter also leads to an underestimation of precipitation events, comparable to the described mixing error.

Higher oscillation thresholds increase the risk of filtering oscillations that represent real processes (e.g. dew formation). The threshold has to be chosen as large as necessary (to filter noise) and as small as possible (to retain slow processes and to prevent the underestimation during rain events). This idea is reflected by the subsequently described adaptive methods, attempting to optimize this parameter with respect to signal. Beside the use of these techniques, we applied the oscillation threshold filter to derive a possible range for the cumulative water balance by selecting a maximum and a minimum value for the possible threshold. As minimum value, we used a threshold of 0 g, implying that every remaining oscillation is interpreted as real effects. To determine a maximum threshold, we investigated the fluxes of the different lysimeters during night time conditions and selected the threshold at a height, where nearly all of these night-time-oscillations vanished. For our data set, we ended with a maximum value of 50 g. This implies, that for the maximum threshold, only processes, which contribute with a minimum of 0.05 mm to the cumulative flux are considered in the water balance. While the use of the minimum threshold will lead to an overestimation of the cumulative fluxes of P and ET, the use of the maximum threshold will cause an underestimation of these values. We therefore assume to find the true values in between these limits.

2.3.2 Parameter adaptation using an estimate of the signal strength

Peters et al. (2014) suggest to adapt the parameters for the smoothing window length and the oscillation threshold to the signal strength in the data. The idea behind this method is to increase the smoothing time window and the oscillation threshold in peri-

HESSD
12, 569–608, 2015

ods where the signal strength is low and the noise is becoming more dominant and to reduce them in situations where noise is less relevant. In their Adaptive Window and Adaptive Threshold (AWAT) filter algorithm, Peters et al. (2014) estimate the signal strength by applying a polynomial fit to the data within a predefined time window. The deviation of the data to the polynomial fit leads to a measure of the signal strength. This estimate is used to adapt the time window for smoothing as well as the oscillation threshold to the signal strength. The parameters are varied in a range between a minimum and a maximum value, predefined by the operator. For the oscillation threshold, Peters et al. (2014) suggested to choose the maximal resolution of the weighing system as minimum value. For our data set, we chose a minimum value of 10 g (respectively 0.01 mm). The further values applied for the AWAT-filter are listed in Table 2 together with the parameters applied in the filtering approach using parallel lysimeters as described in Sect. 2.3.3.

2.3.3 Parameter adaptation using parallel lysimeters

This method uses the combined information derived from a set of parallel lysimeters for the adaptation of the oscillation threshold to the measuring situation. While external forcing by precipitation or evapotranspiration should lead to synchronous reactions of the different lysimeters, the erroneous oscillations are randomly distributed. To eliminate these fluctuations, the fluxes of the different lysimeters are compared at each data point. The adaptation of the threshold is done in a recursive procedure, starting with a minimum threshold value for the whole data period. After the calculation of the fluxes with the actual threshold values, the fluxes between the parallel lysimeters are compared. At each data point, where the individual lysimeters of the set show different signs in the calculated fluxes, the threshold is raised by one step. After the comparison at each data point, the recursion starts again with calculating the fluxes with the updated (now time dependend) threshold values. The recursion ends when the signs of the calculated fluxes are equal or a maximum threshold value is gained. This leads to a good reduction of noise in periods of fluctuations while maintaining the detailed dy-

HESSD
12, 569–608, 2015

namics of processes, where the lysimeter masses show a distinct trend without random oscillations. In our study, we use an algorithmic comparison of six lysimeters, according to one hexagon of a SoilCan test site. To prohibit that one single lysimeter that may not react optimally, which would prevent the registration of small fluxes, we implemented the algorithm such that only an agreement of five lysimeters in the sign of the calculated fluxes is necessary, to prevent a lifting of the threshold in the recursion process. For our calculations we used a step width of 0.01 mm for the recursion, starting with a minimum threshold value of 0.01 mm to a maximum of 0.20 mm (see also Table 2). We refer to this method as synchro-filter.

3 Results and discussion

3.1 Flux dynamics

The influence of the different processing steps on the calculated fluxes on one example lysimeter is illustrated in Fig. 5. While the manual filter and the threshold filter succeed in eliminating large erroneous fluxes (Fig. 5b and c), the subsequent processing steps (Fig. 5d–f) lead to a pronounced reduction of small errors and noise. Because the filtering steps work on different scales, we zoom into the data for a good illustration of the effects.

To examine the remaining variability between the lysimeters after the data processing, we compared the calculated precipitation fluxes for the different lysimeters. As a first part of that comparison, the mean and the range of the calculated fluxes at the soil-atmosphere interface of all 12 crop lysimeters have been calculated (we omitted the grass lysimeters in this consideration because of the different transpiration). The good accordance is illustrated in Fig. 6. The highest variation with a range of 4 mm h^{-1} corresponds to the event with the maximum precipitation rate of 20.2 mm h^{-1}.

HESSD
12, 569–608, 2015

3.2 Temporal resolution

The ability of preserving detailed dynamics and a good temporal resolution by using the basic filtering scheme becomes obvious when looking at the calculated fluxes. Figure 7a shows a heavy rainfall event on 9 Mai 2013 with a duration of only about 20 min, which would be smeared out to a moderate rainfall by applying larger averaging times. A light and short rainfall on 4 Mai 2013 in between situations of evapotranspiration is displayed in Fig. 7b. Larger averaging times would lead to a merging of ET fluxes and precipitation fluxes. Finally, Fig. 7c and d illustrates the intense dynamics of precipitation events in the examples of a medium rainfall event in the period from 26 to 28 April 2013 and a light rainfall from 12 April 2013. A large part of this dynamics would be blurred with an averaging time of more than one hour.

3.3 Cumulative precipitation

For investigating the accuracy of the determined fluxes, the cumulative precipitation for all 18 lysimeters at the Bad Lauchstädt site was calculated for the minimal and the maximal oscillation threshold. The range between the mean values for these two cases was plotted together with the measurement of the nearby raingauge (Fig. 8). The indicated filter uncertainty is representing the range of uncertainty, which results from the contrary influences of noise error and mixing error, and was calculated by using the minimal and maximal threshold as described in Sect. 2.3.1. This consideration leaves us at the end of the data time series with a cumulative precipitation of (158.2 ± 3.2) mm, indicating a remaining uncertainty of only 2 %. Besides the filtering uncertainty, the variety in the calculated precipitation between the different lysimeters gives us a more integrated picture of the informative value of the estimated precipitation for field purposes. This variety can be caused by systematic deviations between the systems, unfiltered influences on the different lysimeters or the natural heterogeneity in the precipitation. The SD between the different lysimeters for the cumulative precipitation was about 2.7 % of the total value (independent of the choice of the threshold value). If lysimeter mea-

HESSD
12, 569–608, 2015
High-resolution estimation of water balance components from lysimeters
M. Hannes et al.

surements will be used as basis to estimate precipitation for a larger area, these two uncertainties have to be added, which results in an uncertainty of approx. 5 %. The comparison of the lysimeter results with the raingauge measurements shows a good accordance, with slightly lower values for the raingauge during the largest part of the time series. These lower values can be caused by the known errors of the Hellmann-raingauge system (e.g. Richter, 1995) or by the heterogeneity of the rainfalls and the distance between the measurement devices. Figure 8b shows a comparison of the precipitation on a daily basis.

Figure 9 shows the filter uncertainty together with the results for the adaptive and the basic approach using different parameter selections. In all the approaches, the data was processed with the first three filtering steps (manual filter, threshold filter, median filter) before doing further filtering steps. In the case of an averaging time of 5 min, we also reduced the time window for the median filter to 5 min. Only the approaches with a more extreme choice of the filtering parameters (5 and 120 min smoothing window, 100 g threshold) lead to results that are outside the determined uncertainty range. For all the other parameter selections as well as the adaptive methods, the cumulative precipitation is inside the uncertainty range. The difference of the basic approach to the adaptive methods is therefore quite low and does not exceed the 2 % uncertainty. However, this may be due to the fact that the positive effect of remaining noise is compensated partly by a negative effect of the mixing error. If this would be the reason, an underestimation of precipitation during events would go in hand with an overestimation of precipitation during situations of low external forcing. Such a behaviour would lead to deviations in the time-resolved fluxes, even if these errors would cancel out in the cumulative balance.

To furher examine if the more sophisticated filtering approaches (the AWAT-filter, and the synchro-filter) lead to a reduction of both these error components and therefore to a better accuracy of the calculated water balance over the whole time series, a partitioning of the data set into periods with and without precipitation was done. Figure 10 shows the different periods. Rainfalls with a minimum flux rate of 1 mm h^{-1} (blue boxes)

HESSD
12, 569–608, 2015

were chosen such that the selected period starts and ends between 200 and 250 min before and after the registration of positive fluxes. This is to ensure that even the temporal blurring of high averaging times of 180 min will not lead to a smearing of the fluxes out of the selected time window. In these periods of distinct rain, the noise error plays a minor role (because the fluxes are mainly positive and do not oscillate from positive to negative values) and so they can be used to estimate the size of the mixing error. The green boxes indicate very small rainfalls. These periods were excluded from the examination, because in such cases, the mixing error as well as the noise error are relevant. The rest of the data set represents periods of dominat noise and minor mixing error. The only contributions to precipitation are very small processes like dew formation.

For estimating the contribution of the investigated errors we compared the calculated precipitation to a reference value. For the rain periods, where noise is playing a minor role, we used the basic approach with an oscillation threshold of 10 g (corresponding to the weighing accuracy) as reference. This low value prevents distinct influences of the mixing errors, while the noise effect is assumed to be minor. For the no-rain periods, where the mixing of ET and P is less important, we used the basic approach with the maximum oscillation threshold value of 50 g as reference, where nearly all oscillation during night time vanished. Figure 11a shows the deviations to these reference values for different averaging times, without applying an oscillation threshold filter. The deviation during the rain-periods, indicated by the blue line, is an estimate for the mixing error, the deviation during the no-rain periods (red line) is an estimate for the noise error. The noise error is clearly decreasing with increasing averaging time, while the contribution of the mixing error is increasing. For an averaging time of about 50 min, the two errors are compensating each other. For higher averaging times, the mixing error is increasing and leads to a deviation of about 5 mm for an averaging time of 120 min. Averaging time below 20 min (without the use of an oscillation threshold) leads to a strong increase of the noise error.

HESSD
12, 569–608, 2015

In Fig. 11b the influence of the chosen threshold on the error estimates is illustrated. For this examination, we used the basic processing scheme with a fixed time window of 15 min for smoothing together with a variable value for the oscillation threshold. The principle effect of an increasing mixing error with higher threshold values and an increasing noise error for lower threshold values is comparable to the effect indicated in Fig. 11a – but with a much better reduction of noise especially for low thresholds, which is due to the preceding filtering with a fixed averaging time of 15 min. Although a good choice of the smoothing time may lead to a good error reduction, the combination of a short smoothing time and the following oscillation threshold filter further reduces the risk of large error influences. However, the main advantages of using the oscillation threshold filter are the maintenance of a higher temporal resolution (for a better reflection of the process dynamics) and the possibility to get an estimation of the filtering uncertainty in the previously described way. Recapitulating these results, the overall error occuring from the described filtering errors, excluding averaging times below half an hour without using an oscillation threshold filter, contribute to the total water balance with a maximum of about 3 %. For AWAT-filter and the synchro-filter, the resulting error estimates are both indicated in Fig. 11a. Both methods further reduce the errors compared to the range of errors given by the accuracy range and, hence, provide a better estimate. While the estimate for the noise error is less for the synchro-filter (1.1 mm) than for the AWAT-filter (2.2 mm), the AWAT-filter is more effective in avoiding the mixing error during rain periods (0.2 mm AWAT, −1.0 mm synchro). Here it has to be stated, that our reference value is only an estimator for the real value, and the real value for the cumulative precipitation is not known exactly. This is especially important when interpreting the results for the noise error, where some real effects might be misinterpreted as errors. In summary, the adaptive methods seem to achieve a good reduction of the filtering errors for our test data set, but the advantage in comparison to the basic methods seems to be minor. This is especially the case, if we compare the errors to the higher variability between the different lysimeter measurements, which is not dependent on the filter method. Nevertheless, the filtering errors in other data sets may be

HESSD
12, 569–608, 2015

higher because of a greater influence of noise on the data. We therefore recommend to always make an estimation of the uncertainty in the described way by choosing a minimum and a maximum threshold for getting an idea of the possible filtering uncertainty. If this uncertainty range is relatively high, it may be worth to use more sophisticated methods like the AWAT-filter or the synchro-filter to further reduce the uncertainty.

3.4 Cumulative evapotranspiration

The influence of the filtering error that was discussed in the previous chapter for the cumulative precipitation is similar to the cumulative evapotranspiration. An overestimation of P (positive flux) comes along with an overestimation of ET (negative flux), because the total flux at the upper boundary is determined by the absolute mass change of the lysimeter and the seepage water reservoir. Thus, an absolute uncertainty of 3 mm for the cumulative value of P due to filtering uncertainty is implying the same uncertainty for ET. The relative uncertainty is dependent on the absolute value of ET. For the used data sets, the absolute value of ET exceeded the value of P, so that the described filtering uncertainty is even below the value of 2 %.

However, the variance between the different lysimeter measurements is much higher for ET than for precipitation. In Fig. 12 this variance is illustrated as mean and SD for the basic processing approach with an oscillation threshold of 50 g. For this calculation, only the 12 crop lysimeters of the Bad Lauchstädt test site were taken into account, the 6 grassland lysimeters were excluded because of the different transpiration. The resulting SD at the end of the time series is only about 6.5 % of the total. The higher variance may be caused by differences in plant growth as well as by differences in soil properties. This uncertainty (together with the filter uncertainty about 8.5 %) can serve as a first estimate for the uncertainty when using lysimeter measurements for estimating ET for a surrounding field of the same soil and vegetation. This implies the assumption, that the plant development on the lysimeters reflects the plant development in the field at least in the mean, without systematic deviations. To investigate the influence of the soil type, the small figures show the cumulative ET separated by the

HESSD
12, 569–608, 2015

soil origin. Two soils (Sauerbach and Bad Lauchstädt) exhibit considerable differences in the mean evapotranspiration and a reduced variability. Because of the small data basis with only three replicates per soil we refrain from a statistical examination of the influence of the soil type.

3.5 Seepage flux

Strong fluctuations on the seepage mass data are rare. The signal is typically much smoother and mass changes occur slowly. Furthermore, no algorithmic separation in positive and negative fluxes have to be processed, so that the choice of the smoothing and threshold parameters on the seepage flux is negligible and small unfiltered peaks remain uncritical. The filtering of the seepage mass data has mainly to cope with the steps caused by emptying and filling of the seepage water tank, which is processed by the threshold filter (filter step 2). The result of the data processing is shown for one examplary lysimeter seepage tank in Fig. 13. A comparison between the different lysimeters is relinquished because the seepage flux is strongly dependend on the soil type as well as on the detailed control of the pumps at the lower boundary.

4 Conclusions

In this study, we presented a basic filtering scheme to remove the various kinds of errors on the lysimeter weighing data, leading to a falsification of the calculated water balance components. We showed the effectivity of these filter components and investigated the influence of the parameter selection on the accuracy of the calculated water balance components. Furthermore, we used the data set of 18 parallel lysimeters to determine the variability between these measurements and compared it with the filtering uncertainty. For our test data set, we found, that the uncertainty in the cumulative precipitation and evapotranspiration due to the choice of the filtering parameters for noise reduction is only about 2 %. This uncertainty is less than the uncertainty that is given

HESSD
12, 569–608, 2015

Title Page
Abstract | Introduction
Conclusions | References
Tables | Figures
◀| |▶
◀ ▶
Back | Close
Full Screen / Esc
Printer-friendly Version
Interactive Discussion

by the heterogeneity of the precipitation measurements between the different lysimeters, that is 2.7 %. For the use of lysimeter measurements to estimate precipitation in the surrounding field, both uncertainties have to be summed up, which makes a total uncertainty of approx. 5 %. This accuracy can be achieved while maintaining a high temporal resolution of 15 min. Examples were shown, where good temporal resolution is necessary to retain the correct process dynamics. Despite the higher variability in the resulting ET (6.5 %), which may be due to differences in plant growth, this moderate uncertainty below 10 % (after adding both errors) show the potential of using lysimeter measurements as a suitable estimate of field ET with a tolerable uncertainty (what should be investigated in further studies). We further tested two filtering approaches, where the filtering parameters are adapted to additional data information. Both adaptive methods, the AWAT-filter (Peters et al., 2014) and the synchro-filter, showed a good reduction of noise within the uncertainty limits. By using subsets of the data, we further investigated the dependency of the filtering errors on averaging time and oscillation threshold. We showed that the use of averaging times between approx. 30 min and 1 h lead to lowest filtering errors. However, using a combination of a short smoothing time (15 min) together with the oscillation threshold filter, the filtering error could even be further reduced. The AWAT-filter and the synchro-filter both showed a good reduction of both error components. However, the improvement of these methods compared to the basic approach with adequate filtering parameters was only minor.

Acknowledgements. The research was supported by TERENO (TERrestrial ENvironmental Observatories). M. Hannes acknowledges support by the Helmholtz Impulse and Networking Fund through Helmholtz Interdisciplinary Graduate School for Environmental Research (HIGRADE) (Bissinger and Kolditz, 2008). WESS is supported by a grant from the Ministry of Science, Research and Arts of Baden-Württemberg (AZ Zu 33-721.3-2) and the Helmholtz Centre for Environmental Research – UFZ, Leipzig. We thank all the technicians and scientists who account for the realization and maintenance of this large network of lysimeters. We further thank A. Peters for providing the AWAT code and U. Franko for the measurements of the raingauge. We also thank our partners from UMS GmbH, Munich, for their support by solving technical problems. We further thank the “Arbeitskreis Lysimeterdatenauswertung” for the

HESSD
12, 569–608, 2015

fruitful discussions.

The service charges for this open access publication have been covered by a Research Centre of the Helmholtz Association.

References

Bogena, H., Schulz, K., and Vereecken, H.: Towards a network of observatories in terrestrial environmental research, Adv. Geosci., 9, 109–114, doi:10.5194/adgeo-9-109-2006, 2006. 574

Fank, J. and von Unold, G.: High-precision weighable field Lysimeter – a tool to measure water and solute balance parameters, Int. Water Irrig., 27, 28–32, 2007. 572

Forster, F. and Baumgartner, W.: Determination of rare rainfall intensities of short-duration-case studies compared with maps of intense rainfall in Switzerland, Schweiz. Z. Forstw., 150, 209–218, 1999. 574

Grunow, J.: Variationen der Niederschlagsstruktur und ihre meßtechnische Erfassung, in: Publications of the International Association of Scientific Hydrology, Louvain, 285–299, 1960. 574

Meissner, R., Seeger, J., Rupp, H., Seyfarth, M., and Borg, H.: Measurement of dew, fog, and rime with a high-precision gravitation lysimeter, J. Plant Nutr. Soil Sc., 170, 335–344, 2007. 573

Nolz, R., Kammerer, G., and Cepuder, P.: Interpretation of lysimeter weighing data affected by wind, J. Plant Nutr. Soil Sc., 176, 200–208, 2013a. 573

Nolz, R., Kammerer, G., and Cepuder, P.: Verbesserung der Auswertung von Lysimeter-Wiegedaten, Bodenkultur, 64, 27–35, 2013b. 573

Nolz, R., Cepuder, P., and Kammerer, G.: Determining soil water-balance components using an irrigated grass lysimeter in NE Austria, J. Plant Nutr. Soil Sci., 177, 237–244, doi:10.1002/jpln.201300335, 2014. 573

Peters, A., Nehls, T., Schonsky, H., and Wessolek, G.: Separating precipitation and evapotranspiration from noise – a new filter routine for high-resolution lysimeter data, Hydrol. Earth

Syst. Sci., 18, 1189–1198, doi:10.5194/hess-18-1189-2014, 2014. 571, 573, 574, 582, 583, 591

Pütz, T., Kiese, R., Zacharias, S., Bogena, H., Priesack, E., Wollschläger, U., Schwank, M., Papen, H., von Unold, G., and Vereecken, H.: TERENO-SOILCan – Ein Lysimeter Netzwerk in Deutschland, in: 14. Gumpensteiner Lysimetertagung 2011, Raumberg-Gumpenstein, 5–10, 2011. 574, 575

Richter, D.: Ergebnisse methodischer Untersuchungen zur Korrektur des systematischen Messfehlers des Hellmann-Niederschlagsmessers, vol. 94, Deutscher Wetterdienst, Offenbach a. M., 1995. 586

Robison, W. L., Stone, E. L., and Hamilton, T. F.: Large plate lysimeter leachate collection efficiency for water being transported from soil to ground water, Soil Sci., 169, 758–764, 2004. 572

Schrader, F., Durner, W., Fank, J., Gebler, S., Pütz, T., Hannes, M., and Wollschläger, U.: Estimating precipitation and actual evapotranspiration from precision lysimeter measurements, Proced. Environ. Sci., 19, 543–552, 2013. 573, 576, 578, 581

Vaughan, P. J. and Ayars, J. E.: Noise reduction methods for weighing lysimeters, J. Irrig. Drain. E.-ASCE, 135, 235–240, 2009. 573

Vaughan, P. J., Trout, T., and Ayars, J.: A processing method for weighing lysimeter data and comparison to micrometeorological ETo predictions, Agr. Water Manage., 88, 141–146, 2007. 573

Young, M., Wierenga, P., and Mancino, C.: Large weighing lysimeters for water use and deep percolation studies, Soil Sci., 161, 491–501, 1996. 572

Zacharias, S., Bogena, H., Samaniego, L., Mauder, M., Fuß, R., Pütz, T., Frenzel, M., Schwank, M., Baessler, C., Butterbach-Bahl, K., Bens, O., Borg, E., Brauer, A., Dietrich, P., Hajnsek, I., Helle, G., Kiese, R., Kunstmann, H., Klotz, S., Munch, J. C., Papen, H., Priesack, E., Schmid, H. P., Steinbrecher, R., Rosenbaum, U., Teutsch, G., and Vereecken, H.: A network of terrestrial environmental observatories in Germany, Vadose Zone J., 10, 955–973, 2011. 574

HESSD
12, 569–608, 2015

High-resolution estimation of water balance components from lysimeters

M. Hannes et al.

Table 1. Parameters for the different filters in the basic processing approach that were used as standard. If no other information is given, the calculations refer to these parameters.

Standard parameters for the basic processing approach	
threshold for lysimeter mass changes	$\pm 60\,\mathrm{mm\,h^{-1}}$
threshold for seepage mass changes	$\pm 9\,\mathrm{mm\,h^{-1}}$
median filter window	15 min
smoothing filter window	15 min
oscillation threshold	50 g

HESSD
12, 569–608, 2015

Table 2. Used parameters for the adaptive methods.

	AWAT-filter	Synchro-filter
min. threshold	0.0081 mm	0.010 mm
max. threshold	0.240 mm	0.200 mm
averaging time	1–31 min	15 min (fixed)

HESSD
12, 569–608, 2015

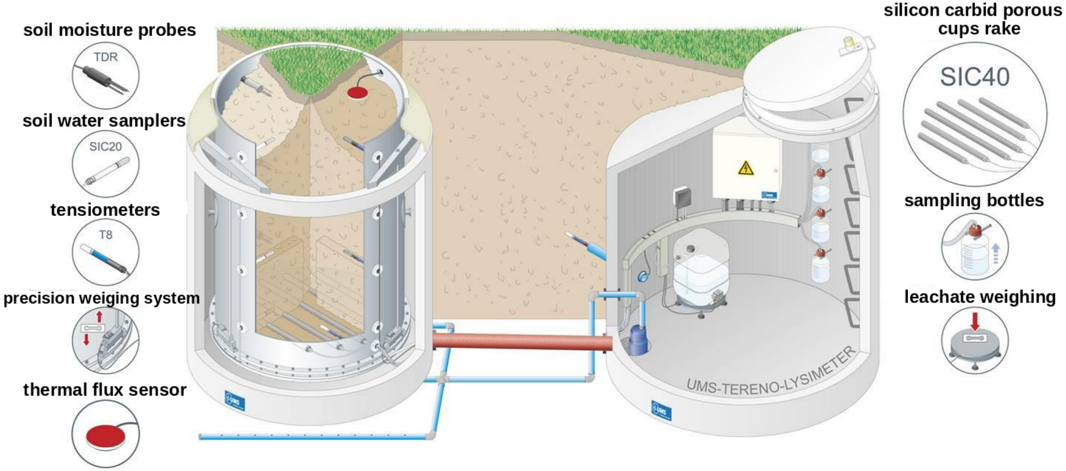

Figure 1. Schematic drawing of a lysimeter (left) as used in SoilCan attached to the central service pit (right).

HESSD
12, 569–608, 2015

Title Page
Abstract | Introduction
Conclusions | References
Tables | Figures
◀◀ | ▶▶
◀ | ▶
Back | Close
Full Screen / Esc
Printer-friendly Version
Interactive Discussion

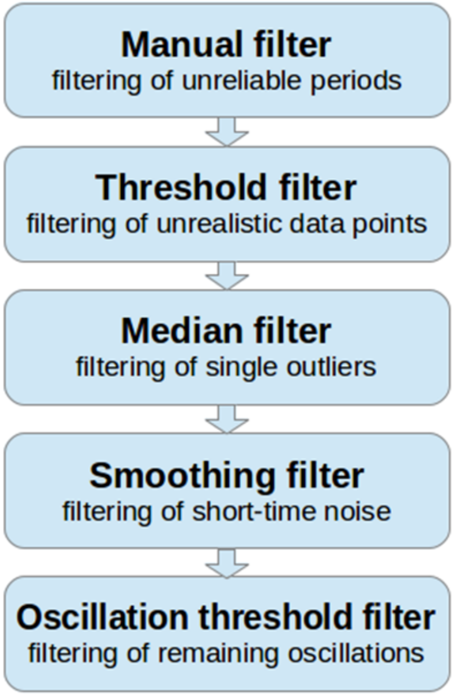

Figure 2. Flowchart of the basic processing scheme.

HESSD
12, 569–608, 2015
High-resolution estimation of water balance components from lysimeters
M. Hannes et al.

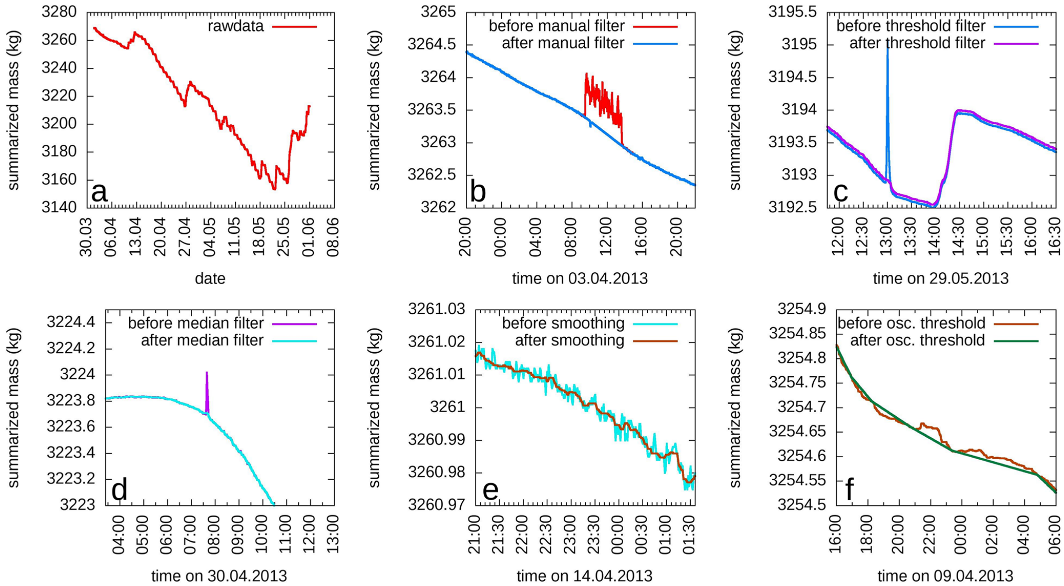

Figure 3. Examples for the effect of the different filtering steps on the mass data (here: summarized mass of lysimeter and seepage water tank of lysimeter BL1-L1). Please note the different scaling of the *y* axes. **(a)** raw data, **(b)** manual filter, **(c)** threshold filter, **(d)** median filter, **(e)** smoothing filter, **(f)** oscillation threshold filter.

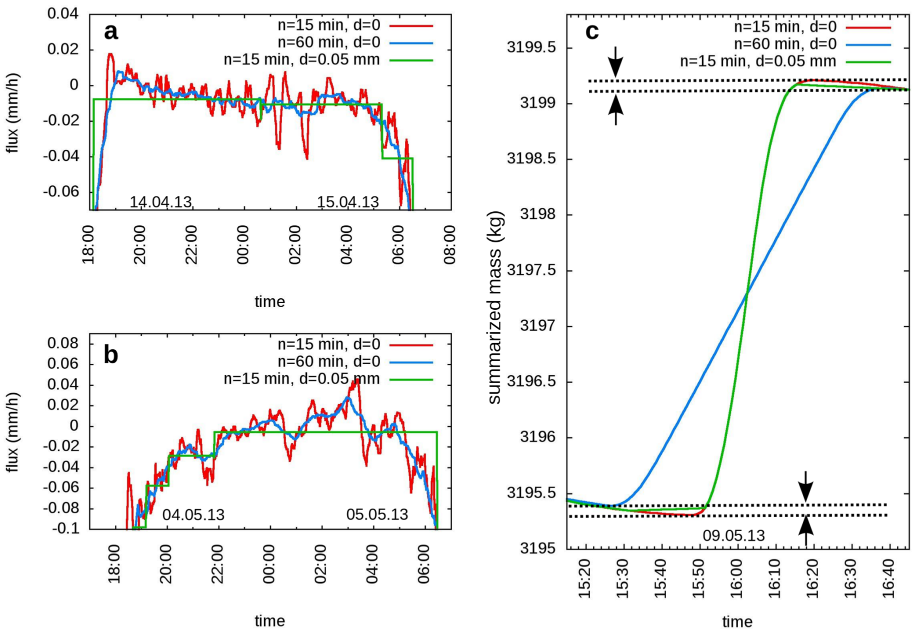

Figure 4. Effects of different averaging time windows n and the oscillation threshold d on the data oscillations (noise error) during night time situations **(a, b)** and the underestimation of precipitation due to the mixing of ET and P (mixing error) during a precipitation event **(c)**. While **(a)** and **(b)** show the calculated fluxes, **(c)** shows the summarized mass of lysimeter and seepage water representing the cumulative flux at the upper boundary. The underestimation of the precipitation induced mass change in **(c)** due to the 60 min smoothing is indicated in the figure.

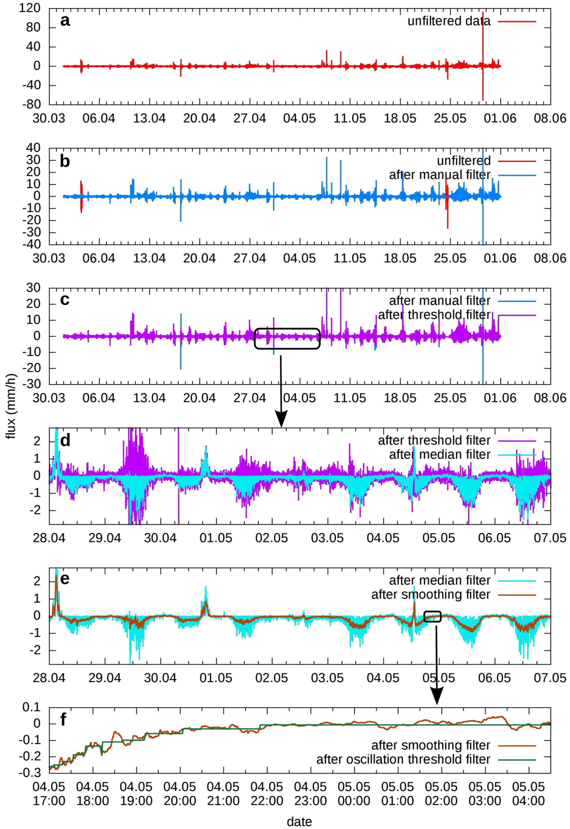

Figure 5. Effect of the different processing steps on the calculated fluxes at the soil-atmosphere-interface for one examplary lysimeter (BL1-L1). After presenting the unfiltered data **(a)**, the effect of the manual filter **(b)**, the threshold filter **(c)**, the median filter **(d)**, the smoothing filter **(e)** and the oscillation threshold filter **(f)** is shown. For **(d)**–**(f)** zoom levels were increased to illustrate the different scales affected by the filtering steps. Please note the different scaling of the axes.

HESSD

12, 569–608, 2015

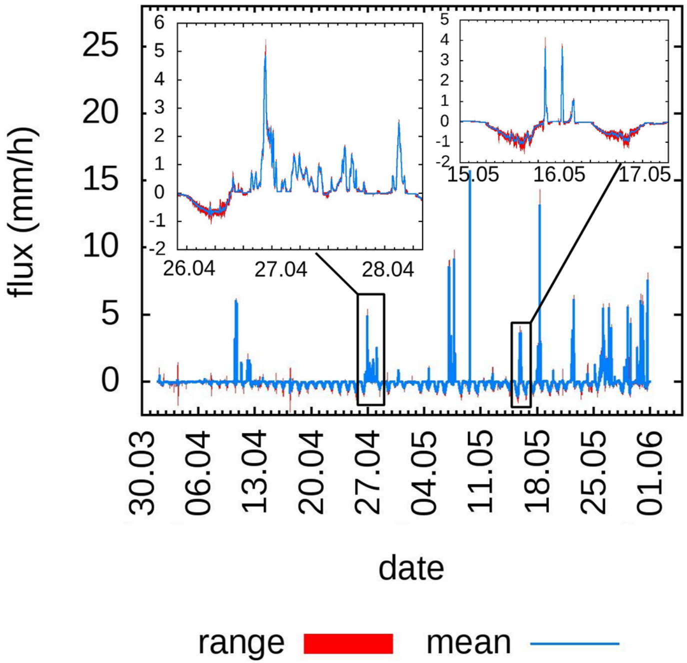

Figure 6. Variations in the calculated fluxes between the different crop lysimeters. The area in red shows the range of minimal and maximal calculations.

HESSD
12, 569–608, 2015

High-resolution estimation of water balance components from lysimeters

M. Hannes et al.

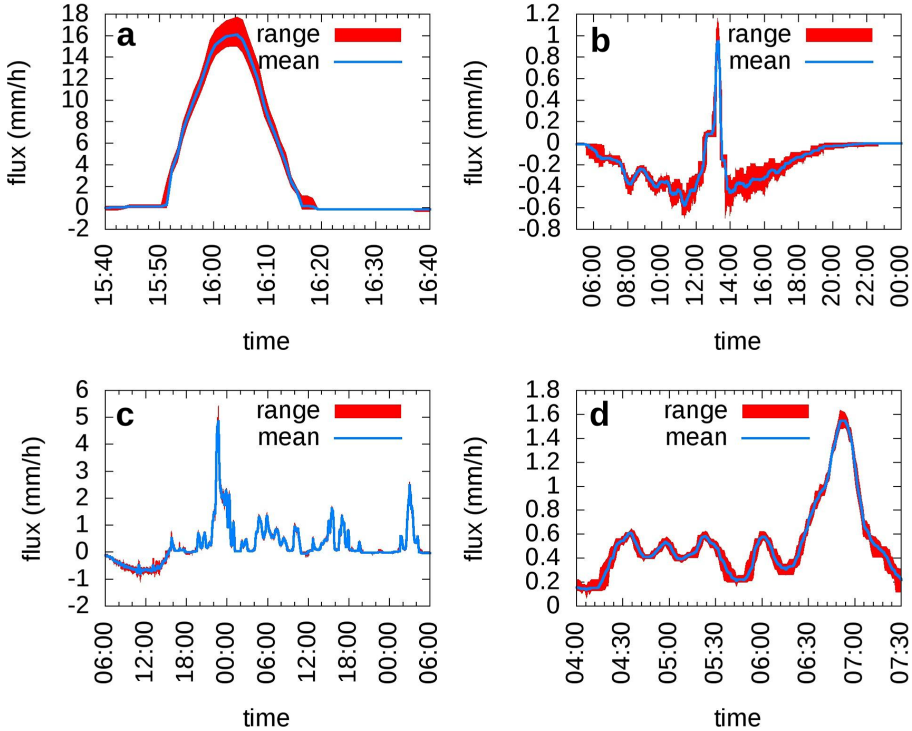

Figure 7. Short time dynamics of precipitation events for selected rain events of 9 May 2013 **(a)**, 4 May 2013 **(b)**, 26–28 April 2013 **(c)** and 12 April 2013 **(d)**.

HESSD
12, 569–608, 2015

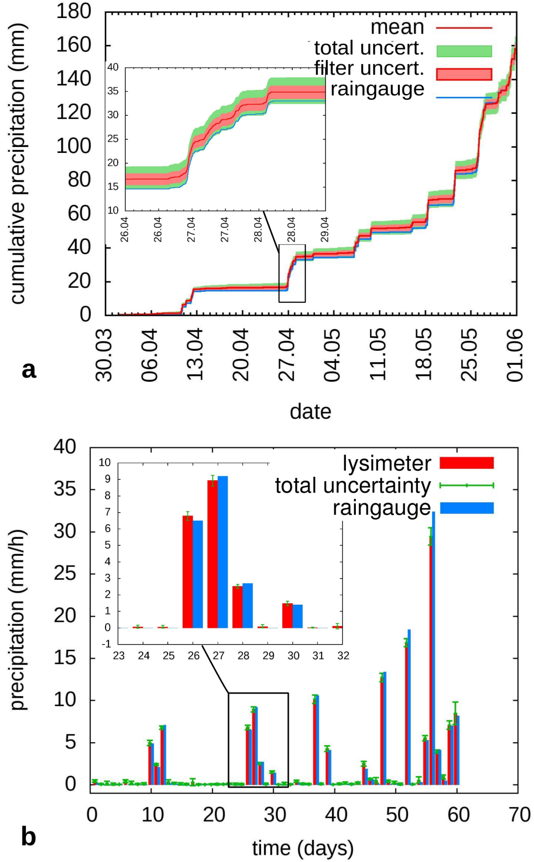

Figure 8. The calculated precipitation with its uncertainties as cumulative precipitation **(a)** and daily precipitation **(b)**. The total uncertainty is the sum of the estimated filtering uncertainty and the SD of the different measurements on the 18 lysimeters.

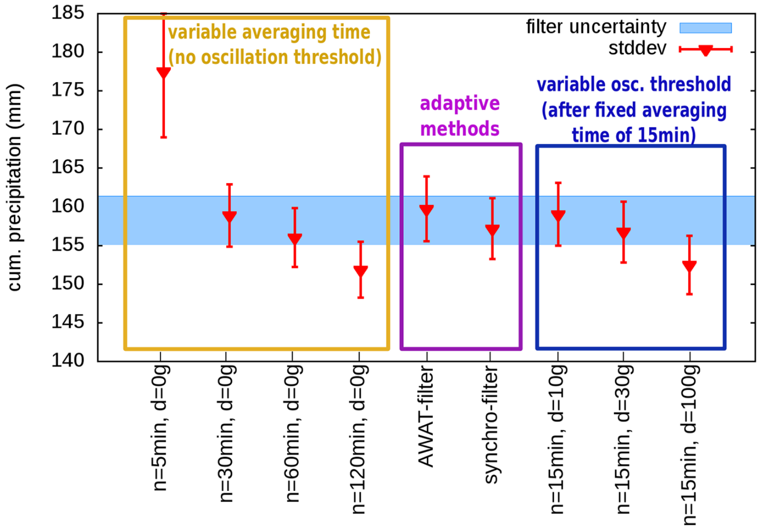

Figure 9. The values for cumulative precipitation together with the SD regarding the measurements of the 18 different lysimeters for different parameter selections and the two adaptive methods.

HESSD
12, 569–608, 2015

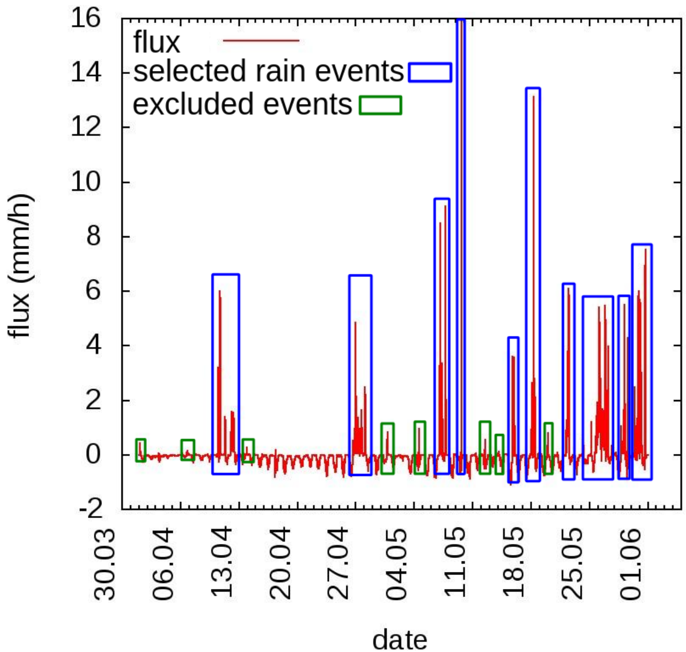

Figure 10. Selection of periods for the investigation of the noise and the mixing error. The purple periods were selected for the estimation of the mixing error, the blue periods of light rain were excluded because of the contribution to both errors and the rest of the data set was used for the estimation of the noise error.

HESSD
12, 569–608, 2015

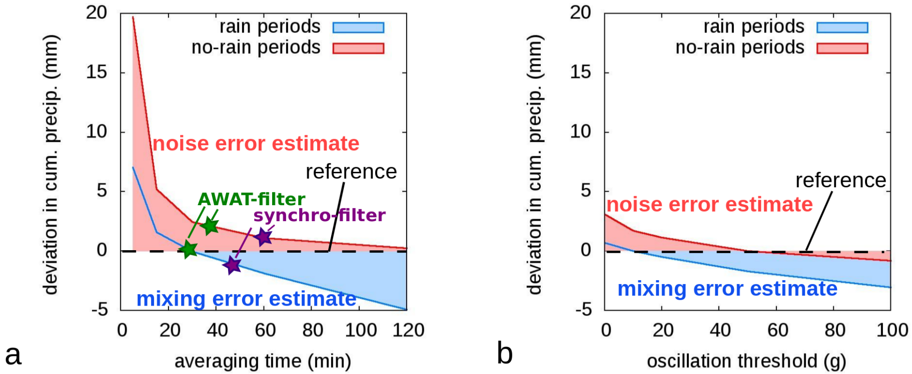

Figure 11. Effects of averaging time **(a)** and oscillation threshold value **(b)** on the estimates for the mixing error and the noise error. The error estimates of the AWAT-filter and the synchro-filter are indicated in **(a)** with green stars for the AWAT-filter and purple stars for the synchro-filter.

HESSD

12, 569–608, 2015

High-resolution estimation of water balance components from lysimeters

M. Hannes et al.

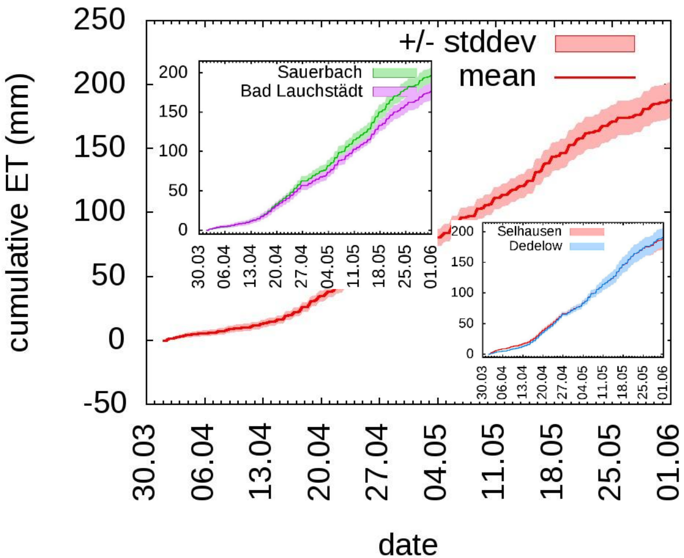

Figure 12. Cumulative Evapotranspiration (mean ± SD) for the 12 crop lysimeters of the Bad Lauchstädt testsite. The small picture shows the results seperated in soil type groups.

HESSD
12, 569–608, 2015

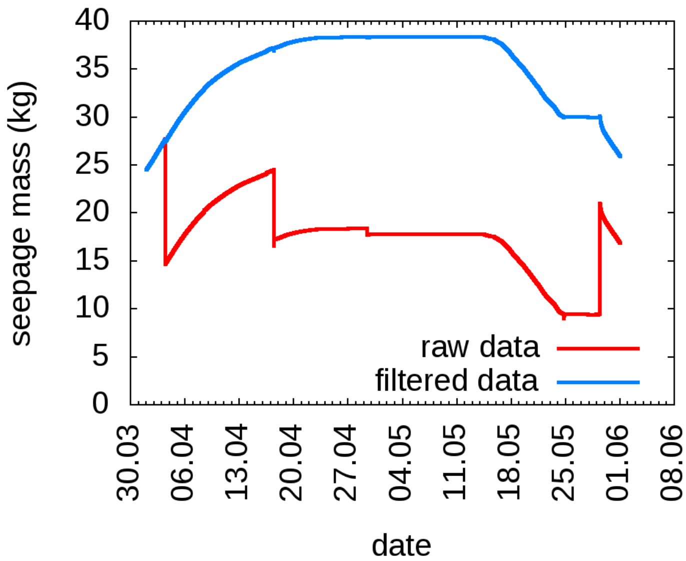

Figure 13. Comparison of processed and raw seepage mass data for the lysimeter BL2-L1.

HESSD
12, 569–608, 2015

High-resolution estimation of water balance components from lysimeters

M. Hannes et al.